MICROSTRUCTURAL EVOLUTION DURING

THERMOMECHANICAL PROCESSING OF ALLOY 625

L. Ferrer, B. Pieraggi and J.F. Uginet *

Laboratoire des Matériaux, ENSCT, 31077 Toulouse, France
* AirForge, 09100 Pamiers, France

Abstract

Wrought nickel - base 625 Alloy is widely used because of its specific combination of fabricability, mechanical properties and corrosion resistance. The primary goal of the present work was to determine the existing relationships between thermomechanical treatments, mechanical properties and corrosion behaviour of Alloy 625. The precipitation diagram for MC, M_6C and $M_{23}C_6$, and δ-Ni_3Nb and γ'' intermetallic precipitated phases was determined. Dynamic and static recrystallisation kinetics and grain growth kinetics were determined as a function of temperature and final strain of thermoechanical treatments. These results permitted to evidence the influence of microstructure on the properties of wrought Alloy 625, and therefore to define the forging routes leading to a given set of mechanical properties and corrosion resistance.

Introduction

Alloy 625 is an austenitic wrought nickel-base alloy containing substantial amounts of chromium (20 to 25 wt%), molybdenum (8 to 10 wt%), iron (5 wt %) and niobium (3.5 to 4.5 wt%) as major addition elements. This superalloy is widely used because of its specific combination of mechanical properties, fabricability and corrosion resistance; it is one of the best corrosion resistant alloy in various media and industrial environments. Alloy 625 is not usually considered as an age hardenable superalloy because of its low content in Al and Ti. However, as a consequence of its content in Fe and Nb (+Ta), precipitation of the metastable, ordered γ'' phase (tetragonal DO_{22}) and δ phase (orthorhombic DO_a) occurs during long term aging of solution treated Alloy 625. Both γ'' and δ phases are based on the composition Ni_3Nb, but with differing stacking sequence of atomically dense planes and differing atomic arrangement of Ni and Nb atoms onto these planes. Therefore, the mechanical properties of Alloy 625 mainly results from solid solution hardening induced by Mo and strain hardening and thus it is not usually employed at temperature higher than about 650 °C.

Only few studies relative to precipitation in Alloy 625 as a function of time and temperature are reported in the open literature (1-6) and no detailed studies of thermomechanical and recrystallization processes are available. In addition, these studies (2-5) mainly deal with the nature of precipitates formed after very long term heat treatments at temperature between 600 and 800 °C and thus are not relevant to usual and practical thermomechanical treatments.

Thus, the aim of the present work was the determination of the thermomechanical processing permitting the control of mechanical properties and corrosion resistance of Alloy 625 forged products for low temperature applications. This goal was partially reached from the TTT precipitation diagram for carbides and intermetallics which precipitates during heat-treatments and thermomechanical processing, and from the recrystalllization processes and kinetics as a function of time, temperature, strain and strain-rate.

Materials and Experimental Methods

The studied alloy was provided by Imphy SA in the form of a forged billet. The average composition is given in Table I.

Table I Composition of Alloy 625 used in this work

Element	Ni	Cr	Mo	Fe	Nb	Co	Al	Ti	Si	Mn	C
Weight %	Bal	20.5	8.2	4.3	3.6	0.1	0.1	0.1	0.1	0.1	0.03
Atomic %	Bal	23.4	5.1	4.6	2.3	0.1	0.2	0.1	0.2	0.1	0.15

The precipitation was studied on specimens solution treated at 1150 °C for 6 hours and water quenched. The precipitation temperarure range was between 600-1075 °C and the heat treatment lasted from 5 mn up to 100 hours. The shortest heat treatments (duration smaller than 2 hours) were performed in a fluidized-bed furnace permitting high heating rate. All heat treatments were performed in air at atmospheric pressure and all specimens were water-quenched after aging.

Thermomechanical treatments were performed on cylindrical bars solutionnized at 1150 °C for 2 hours. The deformation temperature varied between 1050 and 1175 °C and the final true strain ε between 0.25 and 1.5. The ram speed was kept constant and equal to 14 mm.s-1, which roughly corresponds to a logarithmic variation of ε with time.

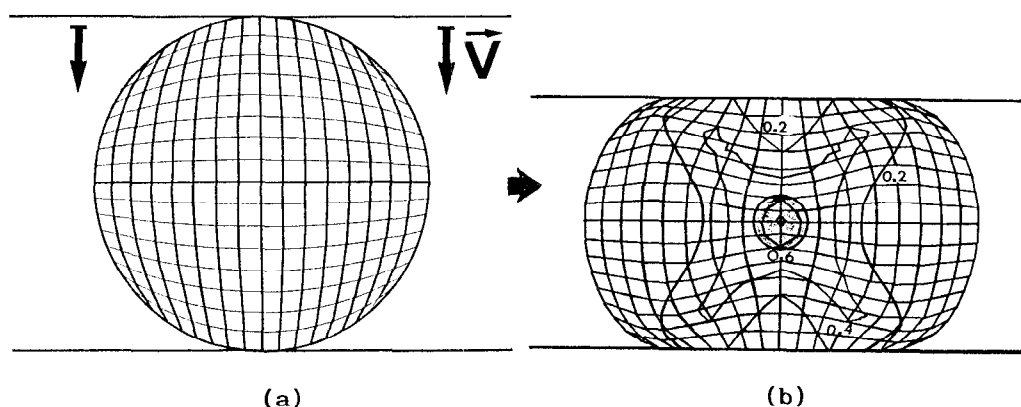(a)   (b)

Figure 1   Simulation of the deformation of a cylindrical bar parallel to its long axis.
- a) Grid before deformation
- b) Same grid after deformation ($\varepsilon_m = 0.63$)

The cylindrical bars were deformed parallel to their longitudinal axis, which minimizes the extent of dead zone in contact with the dies, offers a better reproducibility and leads to a relatively large central zone of homogeneous deformation permitting easy machining of specimens for mechanical testing. Figure 1 a-b shows an example of simulated deformation map used to determine the extent of the central specimen zone homogeneously strained. Local deformations were computed from Vulcain computer program (7). In some case, static recrystallization was studied directly after deformation at temperature between 900 and 1050 °C.

Metallographic examinations were performed on all heat-treated and thermomechanically processed specimens. Specific etching were used to reveal grain boundaries and intergranular carbide precipitates. The mean grain size was determined from the Jeffries' Intercept Procedure (ASTM E112) and the percentage of recristallized phase by planimetry. These examinations were correlated with TEM examinations of thin foils and extraction replicas. Extraction replicas permitted to observe the real shape and morphology of grain boundary carbides and also a semi-quantitative determination of their composition by means of EDX. These analysis were performed on a JEOL 200 CX transmission electron microscope equipped with an EDAX energy-dispersive analyser.

219

Intergranular corrosion tests were performed according to Method A of ASTM G28 test procedure consisting in the measurement of weight loss resulting from the immersion of a test piece of 25x20x3 mm^3 in a boiling solution of concentrated sulfuric acid and ferric sulfate. The measured weight loss after immersion for 120 hours is converted in a uniform corrosion rate expressed in mm per year.

Precipitation in Alloy 625

Precipitates formed after solution heat-treatment and annealing between 600 and 1075 °C were characterized by classical metallography, TEM examinations and EDX analysis of thin foils and extraction replicas.

As usually observed in various austenitic stainless steel and Ni - Base superalloys (8-10), primary carbides (Ti,Nb)C and (Ti,Nb)(C,N) carbonitrides are present after the solution treatment. TEM examinations of extraction replicas permitted to distinguish diamond-shaped and irregularly rounded carbides, but despite their high content inTi and Nb, these diamond-shaped carbides are secondary MC carbides formed during annealing treatments.

Intergranular Secondary Carbides.

Secondary intergranular carbides are formed during annealing treatments. The formation of two different carbides, $M_{23}C_6$ and M_6C, is observed as a function of the annealing temperature. Because of their similar f.c.c cristallographic structure of very close parameters (a = 10.6-10.9 Å for $M_{23}C_6$ and a = 11.1-11.3 Å for M_6C), the precipitation domain of these two intergranular carbides was determined by classical metallographic examinations from the different response of grain boundaries to metallographic etching (Figures 2a and b). Indeed, strong preferential grain boundary dissolution was observed for intergranular carbides formed at temperatures lower than 950 °C while carbides precipitated between 950 and 1075 °C did not induce such a preferential dissolution of grain boundaries.
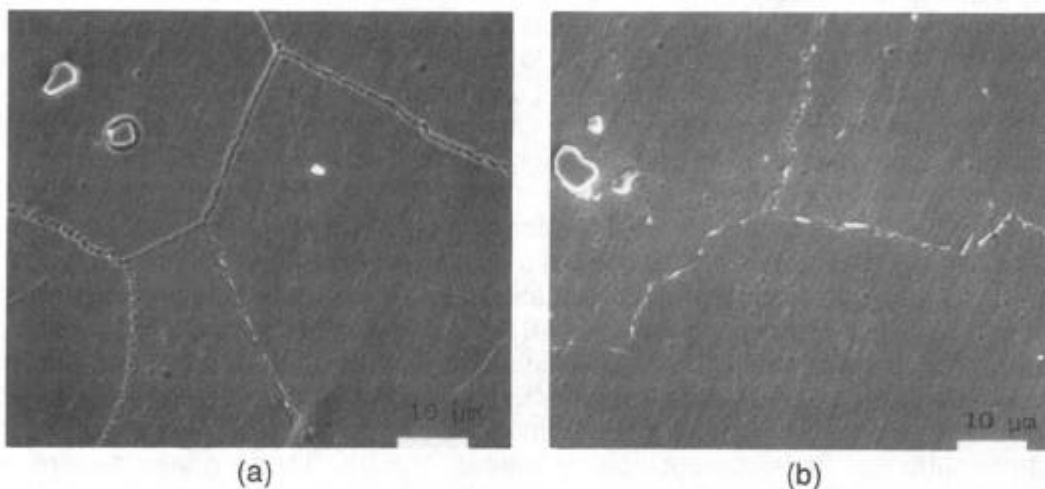

(a)   (b)

Figure 2 - Microstructure of heat treated Alloy 625 : Specimens annealed during 1 hour at : - a) 900 °C ($M_{23}C_6$ major carbide), - b) 1000 °C (M_6C major carbide)

MC carbide precipitates were observed at temperatures between 900 and 950 °C with a dendritic morphology or a diamond shape (Figures 3a and 3b). M_6C carbides were detected after precipitation treatment at temperatures between 1075 and 800 °C, while the precipitation of $M_{23}C_6$ (Figures 3c and 3d) occured at temperatures between 950 and 700 °C. Table II reports some results of EDX analysis performed on differing intergranular carbides ; Mo is the main metallic constituant of M_6C carbides while Cr and Nb are the major elements detected in $M_{23}C_6$ carbides.

(a)

(b)

(c)

(d)
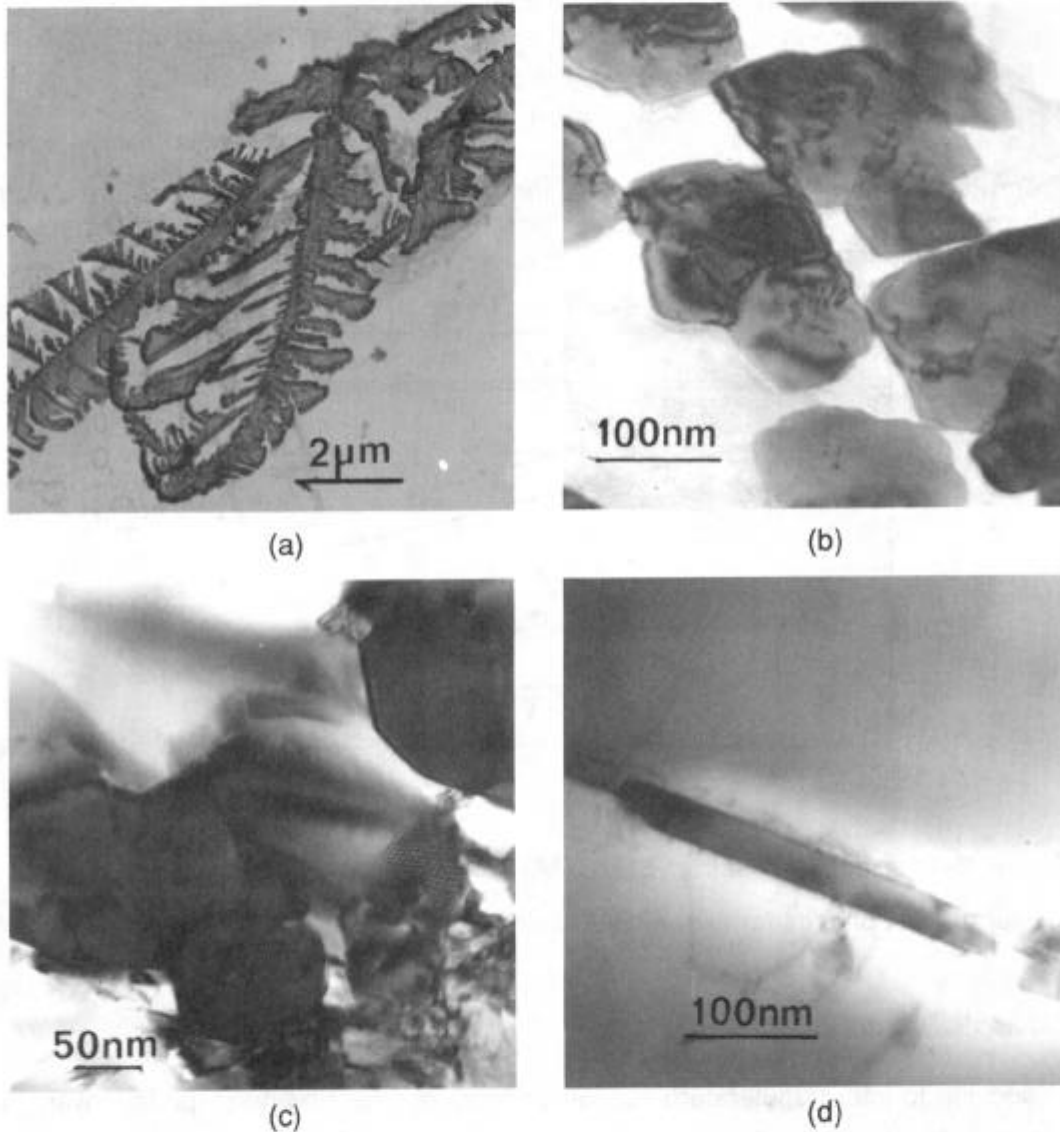
Figure 3 - TEM examination of intergranular carbides :
- a) Dendritic MC (900 °C, 1hr.) - b) Diamond-shaped MC (900°C, 1hr.)
- c) $M_{23}C_6$ (800 °C, 100 hrs.) - d) M_6C (1025 °C, 1hr.).

Table II EDX analysis of extracted carbides (concentrations in atomic percent)

Heat Treatment	Ni	Cr	Nb	Mo	Si	Carbide
700 °C-100 hrs.	10.0	73.0	----	17.0	----	$M_{23}C_6$
800 °C-100 hrs.	8.0	82.0	----	10.0	----	$M_{23}C_6$
800 °C-100 hrs.	44.0	21.4	9.0	25.0	0.5	M_6C
850 °C-15 min.	----	60.0	33.0	7.0	----	$M_{23}C_6$
900 °C-1hr.	----	6.0	75.0	19.0	----	MC
940 °C-100 hrs.	10.0	6.0	75.0	4.0	----	MC
1025 °C-1hr.	26.0	15.0	13.5	40.0	5.5	M_6C

From these observations, the precipitation diagram of carbides was determined as shown by Figure 4. This precipitation diagram is in good agreement with the previous determinations (2-5).
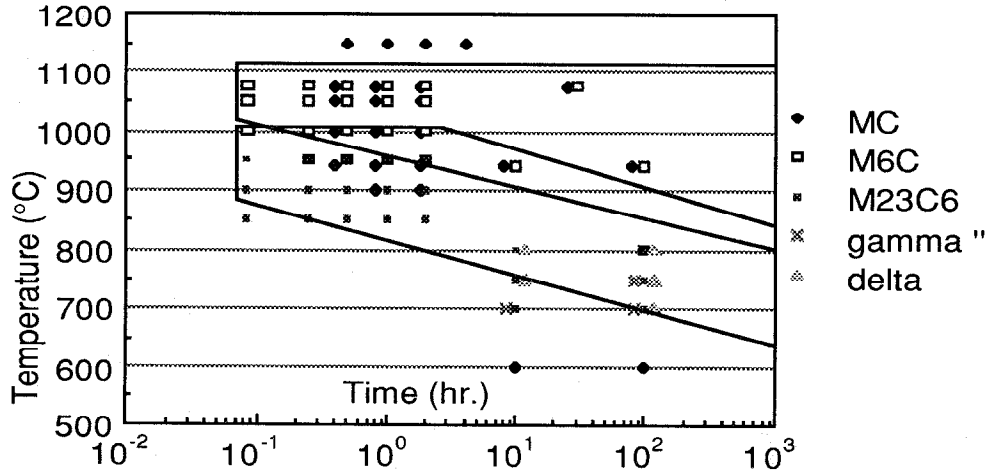

Figure 4 - Precipitation diagram of MC, M_6C and $M_{23}C_6$ carbides, and δ-Ni_3Nb and γ'' intermetallic phases for the studied Alloy 625.

Intermetallic Precipitates.

In addition to intergranular carbides, precipitates of δ Ni_3Nb and γ'' phases were observed after long term aging at temperatures between 650 and 820 °C (Figure 4). The δ phase mainly precipitates in the form of needle, near Nb rich zones often characterized by an important amount of primary NbC carbide (Figure 5a). The δ-Ni_3Nb needles seem to growth from particles of NbC carbide partially dissolved and subsequent diffusion of Nb along the γ/NbC interface (Figure 5b). The precipitation of γ'' is usually heterogeneous and occurs preferentially on dislocations (Figure 5c).
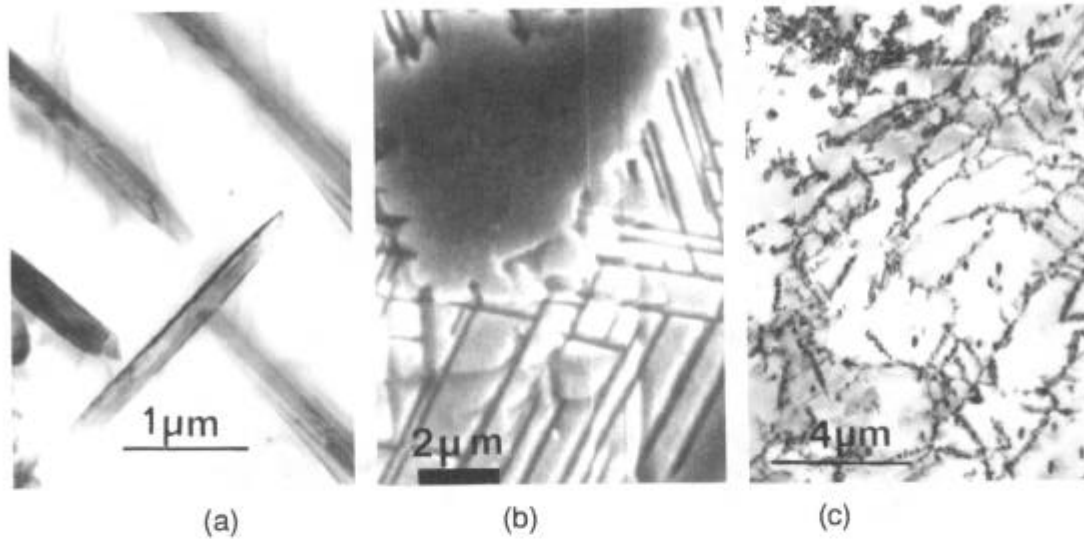
(a) (b) (c)

Figure 5 - Examinations of long term aged specimens of Alloy 625
  - a) δ precipitates formed after aging at 820 °C for 200 hrs.
  - b) δ needles growing from a NbC precipitate.
  - c) γ' precipitates formed after aging at 675 °C for 100 hrs.

The amount of precipitated γ' is small and insufficient to consider the studied Alloy 625 as an age-hardenable alloy as shown by the variation of the yield strength and ultimate tensile stress as a function of temperature for aging times of 10 and 100 hours (Figure 6a). The variation of elongation and area reduction (Figure 6b) is induced by intergranular carbide precipitation.
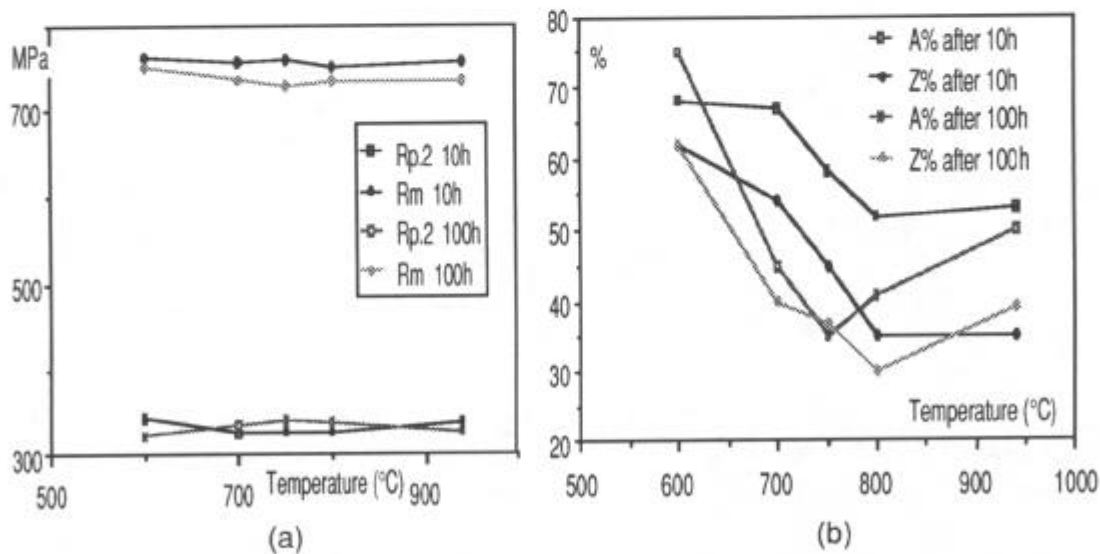

(a) (b)

Figure 6 - Variation of - a) Yield strength (Rp.2)and Ultimate tensile stress (Rm),
  - b) Elongation (A%) and area reduction (Z%), of heat treated Alloy 625
     as a function of aging temperature.

223

Dynamic recrystallization

Figure 7 shows the variation of the fraction of recrystallization as a function of the true strain ε and the deformation temperature. The recrystallization is approximately complete at any true strain for temperatures exceeding 1175 °C. These sets of experimental data can be described by an Avrami equation of the form :

$$R\% = 100 \left[1 - \exp\left(K\varepsilon^n\right) \right] \tag{1}$$

where R% is the percentage of recristallized phase, K and n are constants determined by means of least-square fitting. The continuous curves were drawn from the so-calculated K and n values. The variation of K and n with the temperature is shown on Figure 8.

The value of strain exponent n of Eq. (1) is comprised between 1 and 2, and the constant K between -6 and -2. The n value is in agreement with the ones usually reported for a grain growth control of recrystallization process. This exponent would be approximately equal to 4 in case of a nucleation control. However, these possible theoritical values of exponent n associated to a given recrystallization mechanism must not be considered as a real proof of the occurence of the corresponding mechanism because of the oversimplified hypothesis introduced in the calculations.
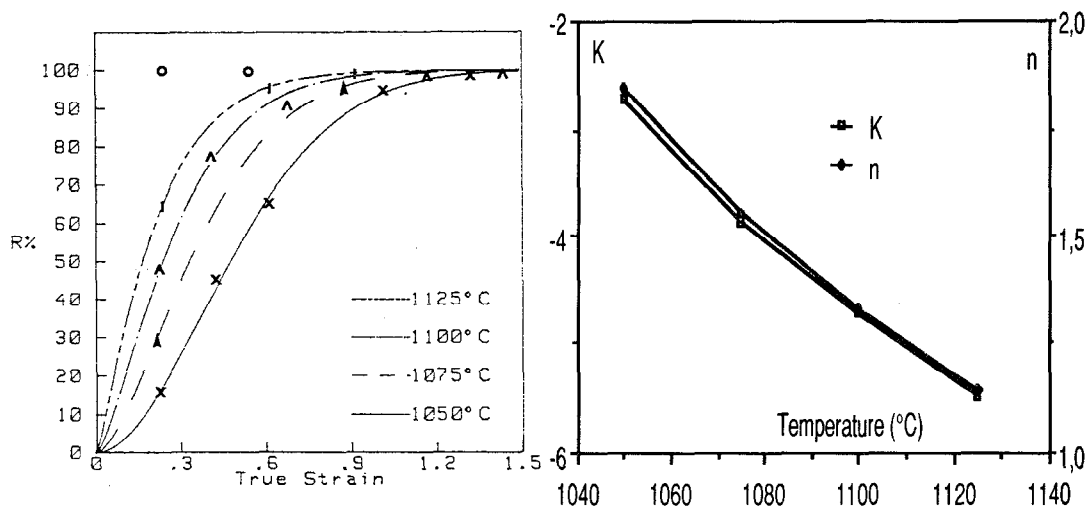

Figure 7 - Variation of the percentage of recrystallization as a function of true strain ε and temperature.

Figure 8 - Variation of the coefficients K and n of Avrami equation describing dynamic recrystallization of 625.

The variation of the average grain size of recristallized material has been determined as a function of deformation temperature and final deformation. The results are reported on Figure 9 for two different final strains of 0.25 and 0.8. The observed variation is approximately linear within the considered temperature range and for

the two reported deformations, which may be interpreted as a control of recrystallization kinetics by the dynamic recrystallization itself.
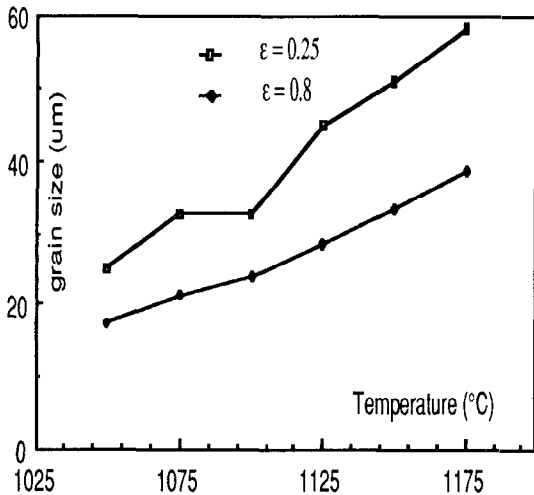

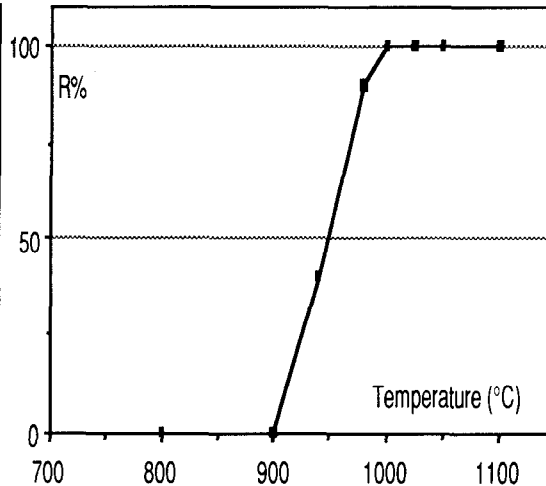Figure 9 - Variation of the average size of recrystallized grains as a function of temperature and final true strain.

Figure 10 - Variation of the percentage of recrystallization R% as a function of heat treatment temperature T.

Static recrystallization

Static recrystallization has been studied as a function of temperature as shown by Figure 10 for an initial deformation ε = o.4 at room temperature and a one hour annealing. This figure show that, under these specific conditions, static recrystallization of deformed specimen of Alloy 625 is observed between 900 and 980 °C. As shown by the presence of some large grains, secondary recrystallization occurs at annealing temperature higher than 1100 °C. Static recrystallization and secondary carbide precipitation interfer as they occur within the same temperature range and are inter-correlated. However, it appears that static recrystallization precedes secondary carbides precipitation, which means that the intergranular carbides could not help to control the grain size of Alloy 625 during thermomechanical processing.

Grain growth

Grain growth was studied between 850 and 1100 °C from the evolution of grain size of specimen annealed for 0.5 and 2 hrs. The initial microstructure of specimens was equiaxed with a mean grain size of 15 - 20 µm (ASTM index 9-10). Figure 11 shows the variation of the mean grain size of annealed specimens as a function of annealing temperature. For the shorter annealing time a sharp increase of grain size occurs at temperatures between 1050 and 1075 °C while the grain size increases over a larger temperature range (940 - 1050 °C) for specimens annealed during 2 hrs.

Plotting log (d^2-d_0^2) as a function of 1/T gives a straight line of same slope for the two annealing times (Figure 12), which indicates that grain growth kinetics are parabolic and thermally activated. The average apparent activation energy is found equal to 225 kJ.mole^{-1}.
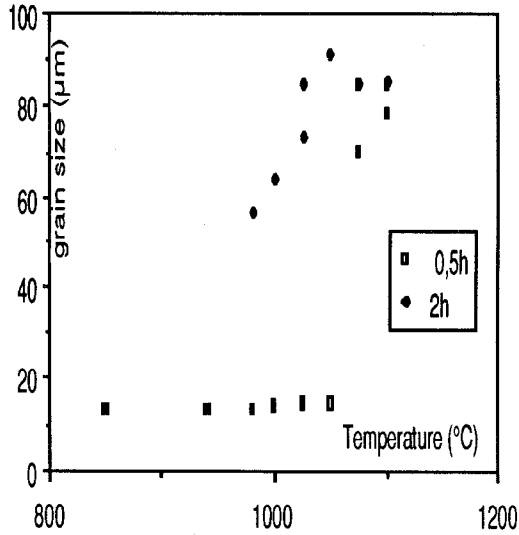
Figure 11 - Variation of mean grain size as a function of annealing temperature.
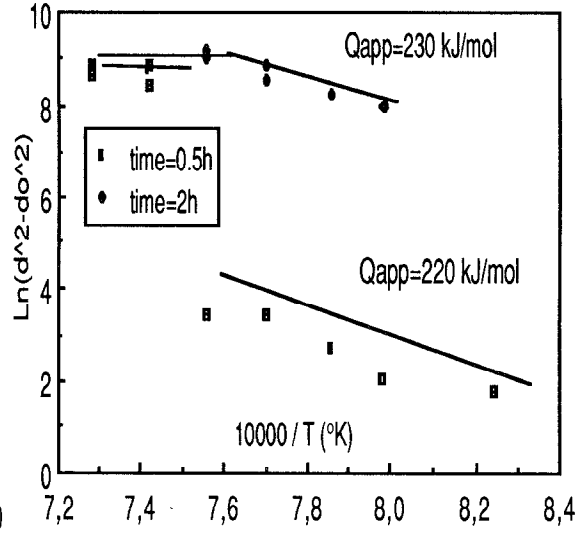
Figure 12 - Variation of $\log(d^2-d_0^2)$ as a function of $1/T(^\circ K)$.

Mechanical Properties and corrosion Behaviour

The primary goal of the present work was to determine the existing relationships between thermomechanical treatments and mechanical properties and corrosion behaviour of Alloy 625.

The relation between microstructure and mechanical properties is well illustrated by Figures 13 a-b showing the linear relationships existing between yield strength and ultimate tensile strength, and the reciproqual square root of recrystallized grain size. These two curves were drawn from data collected on specimens totally recrystallized but submitted to different sequences of thermomechanical treatment.
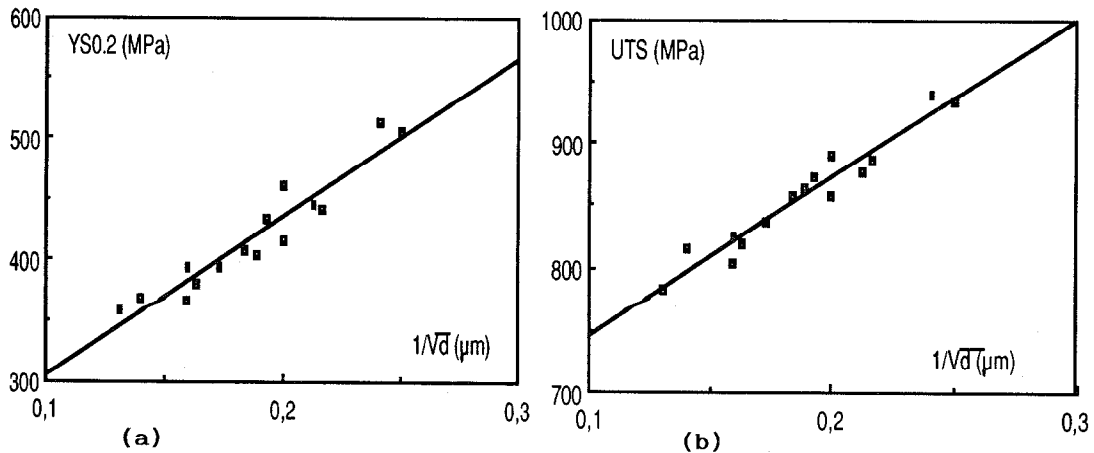

Figure 13 : Variation as a function of $d^{-1/2}$ of a) Yield strength and b) Ultimate tensile stress

226

This $d^{-1/2}$ variation of yield strength and UTS shows the importance of grain size control in thermomechanical processing of Alloy 625. This importance of grain size means that intergranular carbide precipitation are of secondary importance in the control of mechanical properties of forged and recrystallized Alloy 625. Indeed, at approximately constant grain size, different thermomechanical treatments do not induce significant variations of mechanical properties of completely recristallized specimens, most of the observed variations are not significant .

Corrosion behaviour lead to completely differing observations. Figure 14 shows that the variation of the uniform corrosion rate calculated from the weight loss measurements, present a maximun for annealing treatments performed at temperatures between 700 and 850 °C. But, the results of G28 ASTM tests would also depend on the specimen grain size. Indeed, very high value of corrosion rate would be observed as soon as the depth of intergranular attack exceeds the grain size, condition which is more easily fulfilled for fine-grained specimens. Furthermore, a small corrosion rate may correspond to a very deep grain boundary corrosion, particularly in the case of specimens with large grain size.
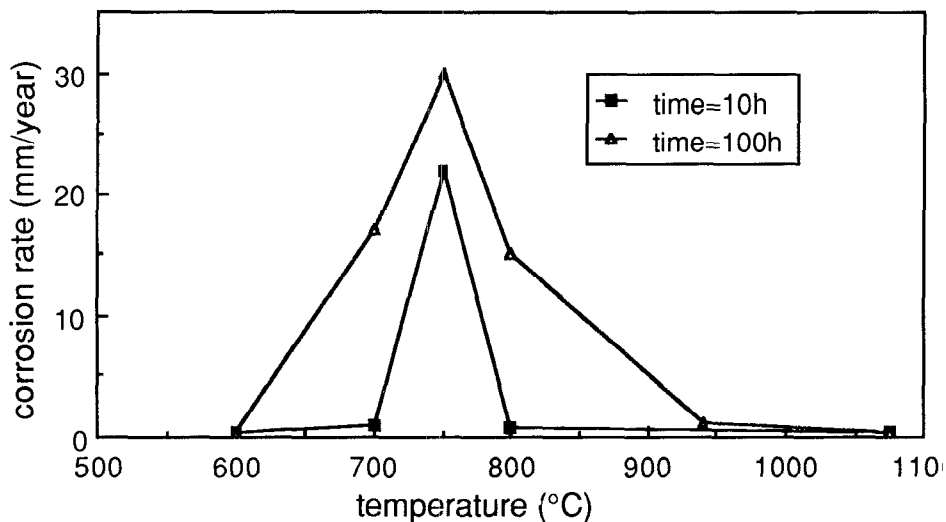

Figure 14 : Variation of corrosion rate deduced from ASTM G28 Test as a function of annealing temperature after thermomechanical processing.

Conclusions

Relative to the thermomechanical processing of Alloy 625, the present work evidenced the importance of the final grain on the mechanical propeties of recrystallized alloy. This effect of final grain size is even more important in the case of the studied alloy because of its low content in Al en Ti. Therefore, precipitation of γ" could not change or improve significantly the mechanical properties of Alloy 625. Similarly, the small amount and the small size of intergranular carbides and δ - Ni_3Nb precipitates do not permit to control the final grain size of forged products.

Furthermore, heat treatments in the temperature range 650 -900 °C has a very detrimental influence on the corrosion behaviour. Surprisingly, intergranular precipitates formed after long term aging at temperature between 800 and 900 °C are not $M_{23}C_6$ carbides, which means that the resistance of Alloy 625 to intergranular corrosion is not only dependent on the precipitation of Cr - rich carbides. Other elements such as Mo might have an important effect on corrosion behaviour.

The temperature of the final solution treatment is a very important parameter relative to the mechanical properties and corrosion behaviour of Alloy 625, as shown by the relationships existing between heat-treatment, specimen microstructure and corrosion behaviour, and the grain size dependence of mechanical properties.

References

1) G.P. Sabol and R. Sticker, "Microstructure of Ni - base superalloys", Phys. Stat. Sol., 35, 11, (1969), 11-52

2) F. Garzarolli, A. Gerscha, and K.P. Francke, "Untersuchungen über das Ausscheidungsverhalten und die mechanischen Eigenschaften der Legierung Inconel 625", Z. Metallkde, 60, 8, (1969), 643 - 652

3) H. Böhm, K. Ehrlich, and K.H. Kramer, "Das Ausscheidungsverhalten der Nickellegierung Inconel 625", Metall. und Technik, 24, 2, (1970), 139 - 144

4) E. Schnabel, H.J. Schüller, and P. Schwaab, "The Precipitation and Recrystallization Behaviour of Ni - Base - Alloy Inconel 625", Practical Metallography, (1971), 521 - 527

5) M. Schirra, "Einfluss des Vorbehandlungszustandes auf das Zeitstandfestigkeits und Kriechverhalten einer matrixhärtenden Ni - Basis - Legierung", Metall. und Technik, 36, 4, (1982), 394 - 401

6) M. Sundararaman, P. Mukhopadhyay, and S. Banerjee, "Precipitation of the δ-Ni_3Nb phase in two nickel base superalloys", Met. Trans., 19A, (1988), 453 - 465

7) J.C. Boyer, F. Chevet, "Calcul par élements finis des écoulements en forgeage ", Mém. Scient. Rev. Met., (1988), 337 - 348

8) M. Dalhen, "Carbide precipitation in superalloys", Superalloys 1984, ed. by M. Gell et al., (Warrendale, PA : The Metallurgical Society, 1984), 449 - 454

9) L.k. Singhal, J.W. Martin, "The nucleation and growth of Widmannstatten $M_{23}C_6$ type carbide in an austenitic stainless steel", Acta Metall., 16, 9, (1968), 1159 - 1165

10) P. Lacombe, B. Baroux, G. Béranger, " Les Aciers Inoxydables ", Editions de Physique, (1990)